[Invited] Towards broadband THz spectroscopy and analysis of subwavelength size biological samples

Theo Hannotte, Louis Thomas, Melanie Lavancier, Sergey I. Mitryukovskiy, Jean-Francois Lampin, Romain Peretti

Towards broadband THz spectroscopy and analysis of subwavelength size biological samples

Théo Hannotte[a], Louis Thomas[a], Mélanie Lavancier[a], Sergey Mitryukovskiy[a], Jean-François Lampin[b], Romain Peretti[a*]

[a]IEMN, CNRS, Centre National de la Recherche Scientifique, University Lille, Centrale Lille, Institut Supérieur d'Electronique du Nord, University Valenciennes, UMR 8520 -IEMN, F-59000, Lille, France

ABSTRACT

The Terahertz (THz) technology has now reached a level of maturation, which allows its uses beyond its core domains of application (telecom and imaging for security or healthcare). Vibrational spectroscopy in the THz range is employed in various fields and is specifically promising in (µ)biology. Indeed, the probed vibrational states extend over several nanometers and give a signature of the sample 3D structure at the nanoscale. This is particularly salient for macromolecules (proteins, DNA and RNA strands etc.) since, on one hand, their 3D structure is very difficult to probe in physiological condition with other techniques, and on the other hand, this structure determines their function and is consequently of utmost importance for the living. A major hurdle still arises when applying THz spectroscopy on biological or macromolecular samples. The samples are generally smaller than the THz wavelength, which requires concentrating the THz field in the sample. Solutions aimed at tackling this challenge by using µ/nano technology of THz field concentration and a proper data analysis will be presented.

Keywords: Terahertz, Biophotonics, time domain spectroscopy, vibrational spectroscopy.

1. INTRODUCTION

During the XVII century, the controversy between D'Alembert [1], Euler [2] and Bernoulli [3] shined the light towards the study of resonant vibrations of objects. This had consequences on a wide range of scales from vibrations of violin's strings to vibration of molecular bonds in infrared spectroscopy. The vibrations eigen frequencies serve as a signature for the size, the stiffness and the structure of a body. The size of a lot of biomolecules e.g. proteins and DNA or RNA strands lies roughly in the range from one to 10 nm, making them biochemical nano-objects with a relative symmetry deriving

* Romain.peretti@univ-lille.fr

from the repetition of monomers. Consequently, the vibrations supported by these biomolecules lie in the broad THz range. E.g., collective motion of DNA base pairs along the DNA backbone [4]. Additionally, since biological macromolecules(MMs) are polar, those vibrations couple to the EM-field. In other words, if spectroscopy in the mid-infrared region probes vibrations associated to localized atom-atom stretches in molecules, THz frequency probes delocalized collective vibrational modes in long molecules like MMs. These resonances can serve as "fingerprint" signatures that reveal their internal structure and vibrational dynamics. There are both theoretical and experimental evidences supporting this perspective [5, 6].

Performing THz spectroscopy was a challenge for decades. Indeed, using the historical Fourier transform infrared spectrometer needs good sources and detectors not available in the THz spectral range. However, spectroscopy in THz frequency range has shown an important development in the last decades. The invention of short pulse lasers and its development up to industrial performances as to progress of semiconductor materials and devices lead to time-domain spectroscopy (TDS). The setup comes from sub-picosocond electrical sampling demonstrated by G. Mourou's group [7], that D.H. Auston improved to THz range using non-linear optics [8] for THz emission and detection. Finally, Grischkowsky et al. [9] introduced the photoconductive antennas as in most of nowadays commercial systems. It uses a benchtop short pulsed (<~100 fs) lasers illuminating a semiconductor at a λ (energy) above the energy band-gap to generates mobile carriers. Effectively, the semiconductor changes abruptly from being an insulator into being a conductor. This leads to a sudden electric current across a biased antenna patterned on the semiconductor and an emission of broadband THz pulse. This pulse goes through the sample and is recombined with a controlled delay together with the original laser pulse onto a photoconductive or electro-optical material acting as detector. This allows access not only to the amplitude but as well to the phases of the THz pulse. This coherent technique shows a very high signal to noise ratio and record a spectrum from 0.2 to 5 THz with a dynamic range of 100 Db in about ten minutes, in commercial apparatus.

Consequently, the use of THz spectroscopy has been proposed for a variety of medical and biological applications. In this proceeding, we will report on major development axes. One of the major issues to solve to enable THz spectroscopy of actual bio-samples is that a lot of them are very small compared to the THz wavelength. Therefore, it is mandatory to enable sub-wavelength confinement of the THz electromagnetic field. We will explain our approach to concentrate the THz field to enable THz spectroscopy of small samples.

2. BROADBAND TERAHERTZ CONCENTRATORS

Although the sensitivity of THz-TDS systems are very high, it is not enough to enable the spectroscopy of a single cell and even more a single virion or protein. To enable the performance of THz spectroscopy on subwavelength samples one needs to concentrate the electromagnetic field in a small volume compared to the wavelength. Such confinement has been a subject of interest in the THz community. To our knowledge, all the approaches exploit the relatively good response of metals in the THz range compared to the visible and infrared. This field enhancement can be achieve using scanning μscopy or integrated photonics.

Scanning THz near-field microscopy set-ups can be classified in two different kinds. The scattering Scanning Near-field Microscopy (s-SNOM) [10, 11], uses the oscillating tip of an Atomic Force μscope (AFM) to concentrate the incident light on its nm-sized apex enabling to probe the dielectric constant of a material at a resolution similar to the apex radius (today's record ~ 15 nm [12]). It can be used as a nano-spectroscopy system [13], for instance in the recent report of the characterization of lactose [14]. Although, in this case, due to a relatively low signal to noise ratio, the resolution is ~2 μm using complex experiments and very long integration time. The laser scanning THz emission or detection μscope (LSTEM or LSTDM) [15] is a TDS system where the sample to probe is directly in contact with a THz non-linear optics detector or emitter. The laser gating this emitter or detector scans the surface of the sample. In this configuration, the spatial resolution is defined by the size of the laser spot on the surface of the non-linear crystal and is ~ 1 μm. Since this setup is built around a TDS setup, the near-field spectroscopy is included. Using this configuration the group of *A. Markelz* recently demonstrated THz near-field spectroscopy of μcrystal of MM, namely lysozyme, photoactive yellow protein and RNA

[16, 17]. These results are clearly the most convincing in the frame of biosamples, however, the recording of a spectrum lasts 6 hours, according to the team.

THz integrated photonics achieved light matter interaction enhancement by confining light or EM radiation by two different ways, broadband or resonantly. A broadband concentrator only uses spatial confinement while resonant devices recycle the light in time, building a stronger field enhancement but on a smaller spectral range.

Most of the broadband approaches use a metallic waveguide such as a parallel plate metallic waveguide [18] because the lowest frequency mode (transverse EM) has no cut-off, is low-losses and low-dispersion. However, this is a 1D waveguide, and besides the drawback of only confining in 1D, using it with a beam induces dispersion and coupling losses. It enabled spectroscopic measurements of thin polycrystalline film of deoxycytidine. The group of E. R. Brown overcame this by setting the sample transversally to the beam. This allowed smaller sample size with a nanofluidic integration enabling the recording of a signature between 850 and 950 GHz of both DNA & RNA molecules in µL samples [19]. Furthermore, we recently demonstrated that the combination of tapered antenna [20] and a planar geometry [21] overcames the losses dispersion and enables a 2D-confinement. The design is presented in Figure 1:

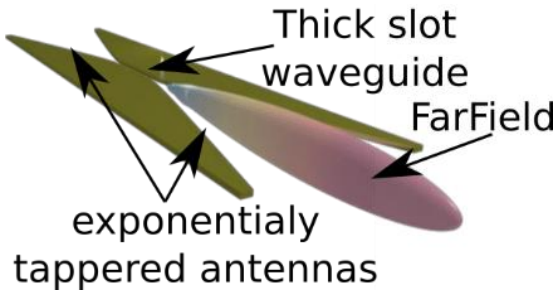

Figure 1: Schematic of the 'butterfly' device showing the waveguide where the sample is to be inserted. The exponentially tapered antenna to couple with the incoming and outgoing THz field and the farfield of the antenna to show the potential of this coupling.

The device, that we named butterfly due to its shape, is designed to fulfil three requirements: (i) An accessible hollow part to insert an sample; (ii) the waveguide should be broadband, low losses and low dispersion (iii) THz-TDS beam should be easily injected & extracted in it. The thick-slot waveguide fulfils (i) & (ii) and the tapered antenna - (iii). We improved the first technology based on laser etching of copper plate to a more rigid and technology compatible material: silicon covered by gold [22, 23]. Thanks to this new technology[24], we succeed in making 20-µm-wide, 300-µm-thick and 1-cm-long waveguide going from a factor 5 [21] in field enhancement to a factor 30 [22, 23]. Consequently, we were able to perform TDS spectroscopy of small amount of powder samples. The first example on α-Lactose is shown in Figure 2.

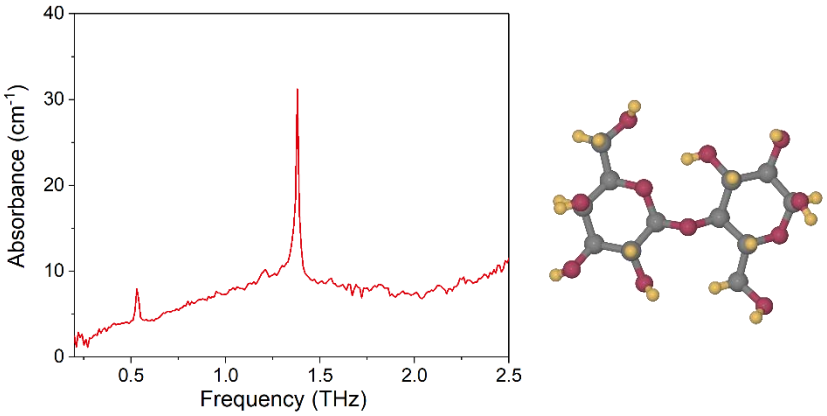

Figure 2: Left - spectrum of a powder of α-Lactose monohydrate. The sample volume is ~ 15 nL corresponding to a mass of ~ 23 µg. Right - schematic view of the lactose molecule.

Here one can see the two well established lactose peaks (e.g. [25]). We continued our study with less usual samples. Amino-acids are the brick from which the proteins are built. We performed the spectroscopy of crystal powder and dried solution of glutamine [$C_5H_{10}N_2O_3$] as shown in Figure 3.

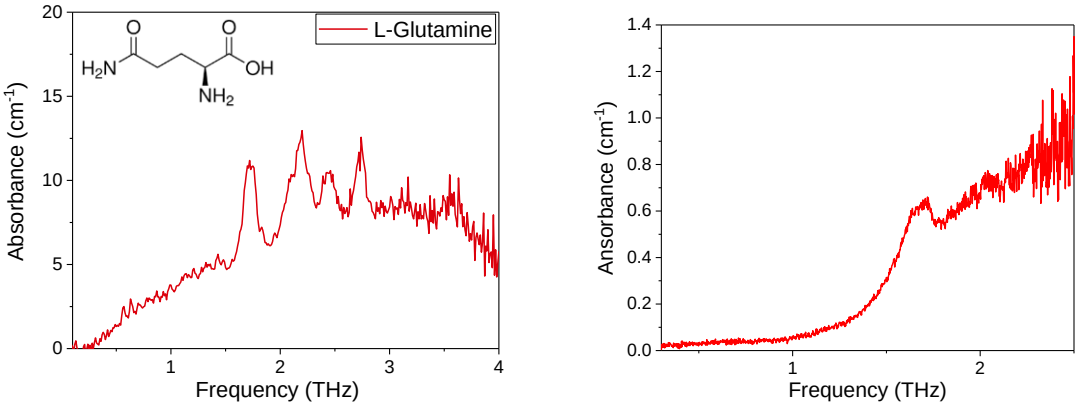

Figure 3: Spectrum of glutamine [$C_5H_{10}N_2O_3$] samples. Left - 6.8 µg of powder (volume of about 5 nL), right - 250 ng of dried solution (volume of dried solution of about 200 pL). We cut the spectrum at 2.5 THz for the dried solution because of the lower signal-to-noise ratio.

On the left figure, one can see four peaks, known for Glutamine molecular crystal, for the sample volume as small as 5 nL, and on the right - only the peak around 1.7 THz is distinguishable, due to losses consequent to scattering. This last spectrum was performed on a 200-pL-volume sample corresponding to a cuboid of about 20 µm by 100 µm by 100 µm. To our knowledge, this is the smallest sample from which a THz spectrum has been extracted. Still, this volume is much larger than the one of a single molecule and one needs to implement better confinement to go towards this goal.

3. THZ RESONATORS

By essence, resonators have a smaller bandwidth but show better concentration. In the THz range, resonators often take the form of metamaterials or metasurfaces coming from radar field and build-up periodic arrangement of sub-λ elements. Typical examples are the dipoles or the split-ring resonator (SRR) [26, 27], where the strong confinement ($V<\lambda^3$) of the

electric field of the resonant mode inside the gap leads to strong field enhancement accordingly to *Purcell* law [28]. These structures are very sensitive to any change in the dielectric constant inside the gap. Thus, sensing based on resonant metamaterials has been studied. THz SRRs enable the detection of extremely small amounts of chemicals [29, 30] and biological substances as spore bacteria and viruses [31, 32]. Recently, the group of *M. Tonouchi* proposed to combine metasurfaces with µfluidic circuitry to set the analyte in a gap sizing ~ 2mm x (10 µm)^2, together with LSTEM to select only a few meta-atoms [33].

SRRs are metallic structures with inductive and capacitive area, thus exhibiting a LC resonance at a wavelength larger than the structure itself. The simplest example is a single metallic loop with a small gap, where the loop itself is the inductive part, and the gap is the capacitive part (see Figure 4). When excited at its resonant frequency, the magnetic field in a SRR is located in the inductive area, while the electric field is confined into the capacitive area. This makes the SRR an excellent tool to confine THz radiation in space (in the gap) and extends the light-matter-interaction time through the resonance.

For our application, we choose the design illustrated in Figure 4. This design has only one capacitive area, allowing for the sake of a better electric field confinement, and two inductive loops. At resonance, the current flows in the two inductive loops in opposite directions, so that the magnetic radiation cancels out in the far-field. This reduces the radiative losses of the device and therefore increases its quality factor. However, we do not want to completely cancel the radiation losses, seeing as they define how the resonator couples with the far-field excitation and measurement. Since we want to test the limit of the field confinement with those resonators, the width of the gap, which defines the final confinement volume, should be an adjustable variable of the design. We therefore use a tapered design that allows to decrease or increase the confinement volume while keeping a constant capacity and thus keeping a constant resonance frequency (see Figure 5).

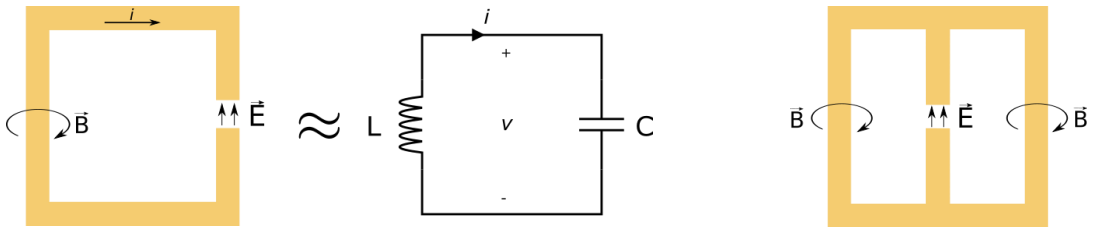

Figure 4: Left: simplest example of SRR with its equivalent circuit, the resonance frequency is given by $\omega_0 = 1/\sqrt{LC}$.
Right: the design we have chosen for our study, the magnetic field inside each loop is oriented in opposite direction.

Figure 5: Left: based on the parallel-plate capacitor model, the capacitance is kept constant by keeping the same ratio A/G. Right: variation of the SRR shape with the two independent parameters (size and gap width).

0. The resonators are made of gold on a 150-µm-thick quartz substrate, which has the advantage of being transparent in both the visible and the THz range. They are fabricated using electron beam lithography according to the following steps (illustrated in Figure 6):Cleaning of a bare quartz substrate using piranha solution to ensure a good hydroxylation of the surface and thus a good adhesion of the resist
1. Coating with a double positive resist layer (PMMA)
2. Deposition of 10 nm Ge layer by electron-beam evaporation to make the sample electrically conductive
3. Electron beam writing of the SRR shape
4. Ge removal using hydrogen peroxide and resist development
5. Deposition of 20 nm of titanium for the adhesion, 200 nm gold
6. Attack on the remaining resist to remove the unwanted and keep only the SRRs (Lift-off)

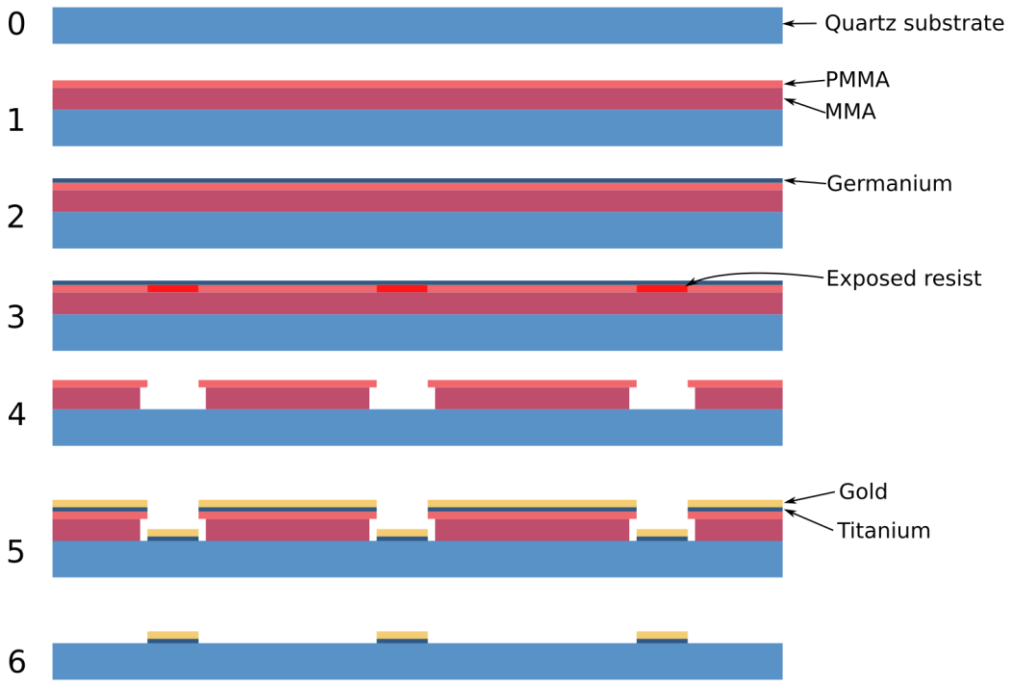

Figure 6: Step by step illustration of the fabrication process.

Using a double resist layer leads to an undercut profile after the development (see Figure 7), resulting in a clean lift-off.

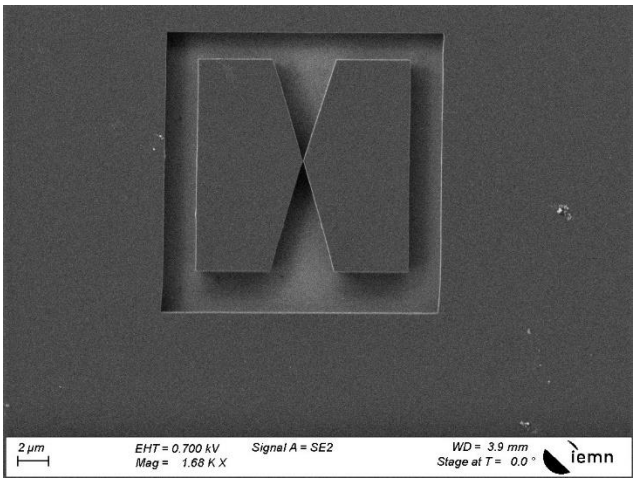

Figure 7: SEM picture of the resist after development (step 4).

As can be seen in the SEM images of the final result in Figure 8, we were able to obtain an excellent agreement with the desired shape and to reach large aspect ratio and very small gap size, down to 30 nm for a total metal thickness of 220 nm.

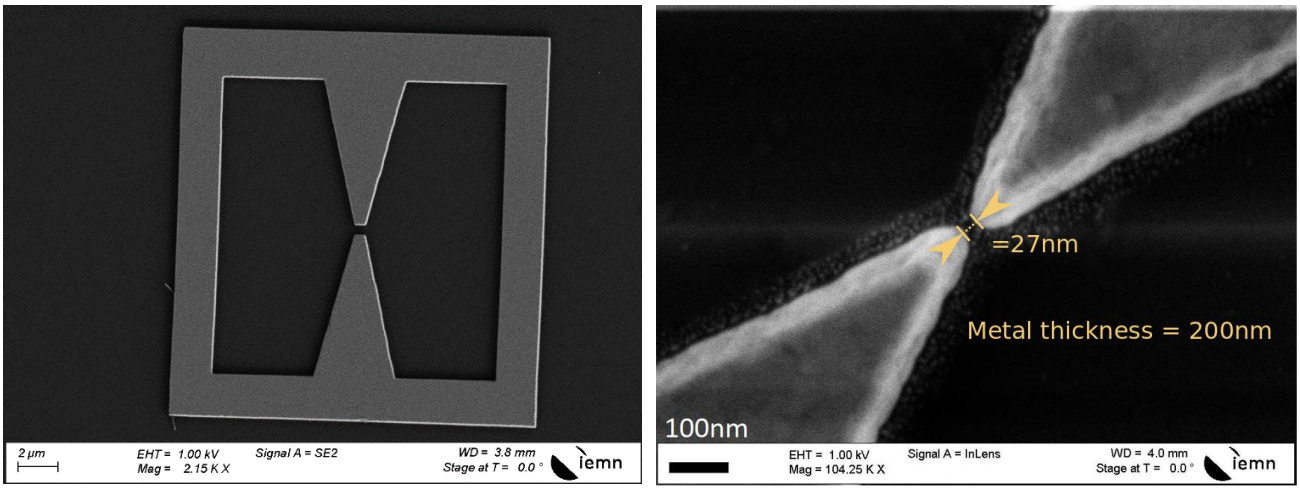

Figure 8: SEM image of a SRR (left) and close up view on a 27 nm gap (right).

The fabricated resonators are characterized with THz-TDS setup, by measuring the transmission of a broadband THz beam through an array of identical resonators. To get a good indication on the resonance frequency of a single resonator, the period of the array must be large enough so that the evanescent near-field of each resonator does not interact with its neighbors. A 50-µm period is large enough according to our simulation, and the array is dense enough to be easily detected with our TDS setup. Although the precise spectral response of a single resonator is not strictly identical to the one measured in an array due to far-field coupling between resonators [34], it still allows us to measure the resonance frequency depending on the two parameters of our resonators (the size and the gap width). Using the frequency response of the quartz alone as a reference, we observe a clear resonance with a quality factor Q ~ 15, which is quite high considering the

deliberately high radiation losses of our device. One can see from Figure 9 right that the tapered shape is very effective in keeping a constant resonance frequency for variable gap width. The spectral characteristics of an array of resonator is in perfect agreement with our expectations.

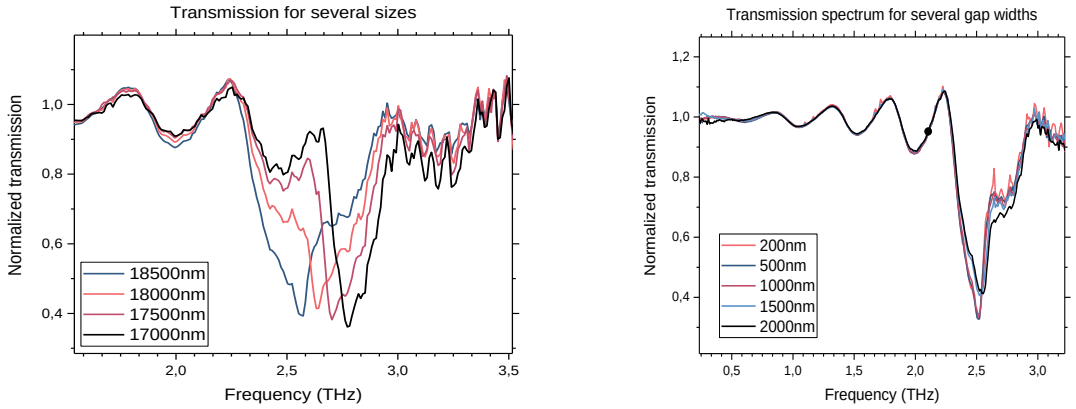

Figure 9: Relative transmission of different arrays of SRR divided by the transmission of a bare quartz substrate, for different resonator sizes (left), and for different gap widths (right).

In order to evaluate our resonator as a way to probe single macromolecule, the next step will be to characterize experimentally the spectral characteristics of a single resonator, and the electric field distribution with SNOM measurement.

4. CONCLUSION

In this proceeding, we briefly presented the methods we are developing to tackle the issue of small-size samples in Terahertz spectroscopy. First, we showed the use of the butterfly device, made of two tapered-antennas to interface a thick-slot metal waveguide toward free space, to enable spectroscopic measurement of sub-nanoliter-volume samples. Then, we explained our strategy and technology to go even further in enabling measurements of samples inside the gap such as of a single split ring resonator.

Still, even when the described technology is mature it will not be enough to be directly useful for biology or biochemistry. First, it will be important to analyze properly the time-trace from the TDS similarly to what was done for free-space experiments such as the metasurface ones [36] for the butterfly. Second, life intrinsically needs water and we need to enable THz spectroscopy in aqueous environment [35] in our device to fulfill this requirement.

REFERENCES

[1] Jean Le Rond d'Alembert. Recherches sur la courbe que forme une corde tendue mise en vibration. *Histoire de l'Académie royale des sciences et des belles lettres de Berlin*, 1(Magasin [R-5]):214–219 & 220–249., 1747.

[2] Leonhard Euler. De vibratione cordarum. *Histoire de l'Académie royale des sciences et des belles lettres de Berlin*, May 1748.

[3] Daniel Bernouilli. Reflexions et éclaircissemens sur les nouvelles vibrations des cordes exposées dans les mémoires de l'académie de 1747 et 1748. *Histoire de l'Académie royale des sciences et des belles lettres de Berlin*, 1751.

[4] A Roggenbuck, H Schmitz, A Deninger, I Cámara Mayorga, J Hemberger, R Güsten, and M Grüninger. Coherent broadband continuous-wave terahertz spectroscopy on solid-state samples. *New Journal of Physics*, 12(4):043017, 2010.

[5] Kuo-Chen Chou. Low-frequency collective motion in biomacromolecules and its biological functions. *Biophysical chemistry*, 30(1):3–48, 1988.

[6] Mauro F. Pereira and Oleksiy Shulika. *Terahertz and Mid Infrared Radiation: Generation, Detection and Applications*. Springer Science & Business Media, 2011.

[7] J. Valdmanis, G. Mourou, and C. Gabel. Subpicosecond electrical sampling. *IEEE Journal of Quantum Electronics*, 19(4):664–667, 1983.

[8] D. H. Auston, K. P. Cheung, and P. R. Smith. Picosecond photoconducting hertzian dipoles. *Applied Physics Letters*, 45(3):284–286, 1984.

[9] M. Van Exter, Ch. Fattinger, and D. Grischkowsky. Terahertz time-domain spectroscopy of water vapor. *Optics letters*, 14(20):1128–1130, 1989.

[10] Xinzhong Chen, Debo Hu, Ryan Mescall, Guanjun You, DN Basov, Qing Dai, and Mengkun Liu. Modern scattering-type scanning near-field optical microscopy for advanced material research. *Advanced Materials*, page 1804774, 2019.

[11] George R Keiser and Pernille Klarskov. Terahertz field confinement in nonlinear metamaterials and near-field imaging. 6(1):22, 2019.

[12] Curdin Maissen, Shu Chen, Elizaveta Nikulina, Alexander Govyadinov, and Rainer Hillenbrand. Probes for ultrasensitive thz nanoscopy. *ACS Photonics*, 6(5):1279–1288, 2019.

[13] Kiwon Moon, Hongkyu Park, Jeonghoi Kim, Youngwoong Do, Soonsung Lee, Gyuseok Lee, Hyeona Kang, and Haewook Han. Subsurface nanoimaging by broadband terahertz pulse near-field microscopy. *Nano letters*, 15(1):549–552, 2014.

[14] Kiwon Moon, Youngwoong Do, Hongkyu Park, Jeonghoi Kim, Hyuna Kang, Gyuseok Lee, Jin-Ha Lim, Jin-Woo Kim, and Haewook Han. Computed terahertz near-field mapping of molecular resonances of lactose stereo-isomer impurities with sub-attomole sensitivity. *Scientific reports*, 9(1):1–8, 2019.

[15] MA Seo, AJL Adam, JH Kang, JW Lee, KJ Ahn, Q Han Park, PCM Planken, and DS Kim. Near field imaging of terahertz focusing onto rectangular apertures. *Optics express*, 16(25):20484–20489, 2008.

[16] Gheorghe Acbas, Katherine A Niessen, Edward H Snell, and AG Markelz. Optical measurements of long-range protein vibrations. *Nature communications*, 5:3076, 2014.

[17] Katherine A Niessen, Mengyang Xu, Deepu K George, Michael C Chen, Adrian R Ferré-D?Amaré, Edward H Snell, Vivian Cody, James Pace, Marius Schmidt, and Andrea G Markelz. Protein and rna dynamical fingerprinting. *Nature communications*, 10(1):1026, 2019.

[18] N. Laman, S. Sree Harsha, D. Grischkowsky, and Joseph S. Melinger. High-resolution waveguide thz spectroscopy of biological molecules. *Biophysical Journal*, 94(3):1010 – 1020, 2008.

[19] W Zhang, ER Brown, M Rahman, and ML Norton. Observation of terahertz absorption signatures in microliter dna solutions. *Applied Physics Letters*, 102(2):023701, 2013.

[20] Alisha J Shutler and D Grischkowsky. Gap independent coupling into parallel plate terahertz waveguides using cylindrical horn antennas. *Journal of Applied Physics*, 112(7):073102, 2012.

[21] Romain Peretti, Flavie Braud, Emilien Peytavit, Emmanuel Dubois, and Jean-François Lampin. Broadband terahertz light–matter interaction enhancement for precise spectroscopy of thin films and micro-samples. *MDPI photoncics*, 5(2):11, 2018.

[22] S. Mitryukovskiy, M. Lavancier, F. Braud, T. Hannotte, E. Dubois, J. Lampin, and R. Peretti. Device for broadband THz spectroscopy of 1-nl-volume samples. In *2019 44th International Conference on Infrared, Millimeter, and Terahertz Waves (IRMMW-THz)*, pages 1–2, Sep. 2019.

[23] Sergey Mitryukovskiy, Mélanie Lavancier, Flavie Braud, Goedele Roos, Théo Hannotte, Emmanuel Dubois, Jean-François Lampin, and Romain Peretti. Shining the light to terahertz spectroscopy of nl-volume biological samples. In *Conference on Lasers and Electro-Optics*, page ATu3K.6. Optical Society of America, 2019.

[24] Sergey Mitryukovskiy, Mélanie Lavancier, Flavie Braud, Yue Bai, Emmanuel Dubois, Jean-François Lampin, and Romain Peretti. Towards broadband THz spectroscopy and analysis of sub-wavelength-size biological samples. In *2019 44th International Conference on Infrared, Millimeter, and Terahertz Waves (IRMMW-THz)*, pages 1–2. IEEE, 2019.

[25] Romain Peretti, Sergey Mitryukovskiy, Kevin Froberger, Anis Mebarki, Sophie Eliet, Mathias Vanwolleghem, and Jean-François Lampin. THz-TDS time-trace analysis for the extraction of material and metamaterial parameters. *IEEE Transactions on Terahertz Science and Technology*, 9(2):136–149, March 2019.

[26] WN Hardy and LA Whitehead. Split-ring resonator for use in magnetic resonance from 200–2000 mhz. *Review of Scientific Instruments*, 52(2):213–216, 1981.

[27] T Hannotte, M Lavancier, S Mitryukovskiy, JF Lampin, and R Peretti. Terahertz radiation confinement using metallic resonators. In *2019 44th International Conference on Infrared, Millimeter, and Terahertz Waves (IRMMW-THz)*, pages 1–2. IEEE, 2019.

[28] E.M Purcell. Spontaneous emission probabilities at radio frequencies. *Phys. Rev. : Proceedings of the American Physical Society*, 69(11-12):674.B.10, Jun 1946.

[29] Yun-Tzu Chang, Yueh-Chun Lai, Chung-Tien Li, Cheng-Kuang Chen, and Ta-Jen Yen. A multi-functional plasmonic biosensor. *Optics express*, 18(9):9561–9569, 2010.

[30] Dong-Kyu Lee, Ji-Hun Kang, Jun-Seok Lee, Hyo-Seok Kim, Chulki Kim, Jae Hun Kim, Taikjin Lee, Joo-Hiuk Son, Q-Han Park, and Minah Seo. Highly sensitive and selective sugar detection by terahertz nano-antennas. *Scientific reports*, 5(15459):15459, 2015.

[31] Audrey Berrier, Martijn C Schaafsma, Guillaume Nonglaton, Jonas Bergquist, and Jaime Gómez Rivas. Selective detection of bacterial layers with terahertz plasmonic antennas. *Biomedical optics express*, 3(11):2937–2949, 2012.

[32] S. J. Park, J. T. Hong, S. J. Choi, H. S. Kim, W. K. Park, S. T. Han, J. Y. Park, S. Lee, D. S. Kim, and Y. H.br Ahn. Detection of microorganisms using terahertz metamaterials. *Scientific Reports*, 4:4988–, May 2014.

[33] Kazunori Serita, Eiki Matsuda, Kosuke Okada, Hironaru Murakami, Iwao Kawayama, and Masayoshi Tonouchi. Invited article: Terahertz microfluidic chips sensitivity-enhanced with a few arrays of meta-atoms. *APL Photonics*, 3(5):051603, 2018.

[34] Lucy L Hale, Janine Keller, Thomas Siday, Rodolfo I Hermans, Johannes Haase, John L Reno, Igal Brener, Giacomo Scalari, Jérôme Faist, and Oleg Mitrofanov. Noninvasive near-field spectroscopy of single subwavelength complementary resonators. *Laser & Photonics Reviews*, page 1900254, 2020.

[35] M. Lavancier, S. Mitryukovskiy, N. Vindas, J. Lampin, and R. Peretti. Retrieving permittivity model parameters for polar liquids and multilayer systems through THz-TDS time-trace data analysis. In *2019 44th International Conference on Infrared, Millimeter, and Terahertz Waves (IRMMW-THz)*, pages 1–2, Sep. 2019.

[36] Romain Peretti, Martin Micica, Sergey Mitryukovskiy, Kevin Froberger, Sophie Eliet, Mathias Vanwolleghem, and Jean-François Lampin. Modeling and parameter retrieving in time domain spectroscopy of material and metamaterial. In *Nonlinear Optics and its Applications 2018*, volume 10684, page 106840P. International Society for Optics and Photonics, 2018.